Dynamical evolution modeling of the Collinder 135 & UBC 7 binary star cluster

Marina Ishchenko[1] **, Peter Berczik**[2,3]
and Nina Kharchenko[1]

[1]Main Astronomical Observatory, National Academy of Sciences of Ukraine,
27 Akademika Zabolotnoho St, 03143 Kyiv, Ukraine

[2]Astronomisches Rechen-Institut, Zentrum für Astronomie, University of Heidelberg,
Mönchhofstrasse 12-14, 69120, Heidelberg, Germany

[3]Konkoly Observatory, Research Centre for Astronomy and Earth Sciences, Eötvös Loránd
Research Network (ELKH), MTA Centre of Excellence, Konkoly Thege Miklós út 15-17, 1121
Budapest, Hungary

Abstract. The purpose of the present work is a detailed investigation of the dynamical evolution of Collinder 135 and UBC 7 star clusters. We present a set of dynamical numerical simulations using realistic star cluster N-body modeling technique with the forward integration of the star-by-star cluster models to the present day, based on best-available 3D coordinates and velocities obtained from the latest Gaia EDR3 data release. We have established that Collinder 135 and UBC 7 are probably a binary star cluster and have common origin. We carried out a full star-by-star N-body simulation of the stellar population of both clusters using the new algorithm of Single Stellar Evolution and performed a comparison of the results obtained in the observational data (like cumulative number counts), which showed a fairly good agreement.

Keywords. galaxies: star clusters, methods: n-body simulations

---

1. Introduction

Recently, based on analysis of positions and kinematic data of Gaia space mission (Gaia Collaboration et al. 2016), several pairs of star clusters showed a probable common origin (for example: Bisht et al. 2021; Pang et al. 2020; Zhong et al. 2019; Kovaleva et al. 2020). Collinder 135 (hereafter Cr 135) and newly discovered (Castro-Ginard et al. 2018) UBC 7 are located in the Vela-Puppis region which attracts active attention since Gaia data allowed to appreciate its complicated history of evolution, space and kinematic structure (Beccari et al. 2018; Cantat-Gaudin et al. 2019b,a; Beccari et al. 2020). We have demonstrated (Kovaleva et al. 2020) that these two clusters locations and velocities suggest that they might have been closer to each other at their initial history, ≈ 50 Myr ago. Backward orbital integration indicates also that the clusters might have been even gravitationally bound in the past, assuming that they were significantly more massive before their violent relaxation (Kovaleva et al. 2020).

We used Gaia DR2 and EDR3 data to restore the most probable members of Cr 135 and UBC 7, using the method presented in Kharchenko et al. 2012. Based on the obtained dataset, we constrain present day parameters of the two clusters, such as space positions, space velocities, masses and density profiles. These data are used further as boundary conditions for star-by-star numerical simulation of dynamical evolution of this pair of star clusters.

Table 1. Initial position and velocity values for Cr 135 and UBC 7 center of mass in Cartesian Galactic coordinates. Taken from `#(53,61)` model, Kovaleva et al. 2020.

Cluster	X, pc	Y, pc	Z, pc	V_x, km/s	V_y, km/s	V_z, km/s
Cr 135	-1061.421	-8382.545	-22.70332	-230.559	33.1769	5.52892
UBC 7	-1065.137	-8386.942	-14.5731	-230.792	34.0251	5.86780

2. N-body modeling of the star clusters evolution

2.1. *Numerical method*

We used the $\varphi-$GPU code for the numerical solution of the equations of motion. The $\varphi-$GPU package uses a high order Hermite integration scheme and individual block time steps (the code supports time integration of particle orbits with schemes of 4th, 6th and even 8th order). Such a direct N-body code evaluates in principle all pairwise forces between the gravitating particles, and its computational complexity scales asymptotically with N^2. We refer the more interested readers to a general discussion about different N-body codes and their implementation in Spurzem et al. 2011a, Spurzem et al. 2011b.

The $\varphi-$GPU code is fully parallelized using the MPI library. This code is written from scratch in `C++` and is based on earlier CPU serial N-body code, Nitadori and Makino 2008. The MPI parallelization was done in the same j particle parallelization mode as in the earlier $\varphi-$GRAPE code, Harfst et al. 2007. The current version of the code uses a native GPU support and direct code access to the GPU's using the NVIDIA native CUDA library. The multi GPU support is achieved through global MPI parallelization. Simultaneously, our code effectively exploits also the current CPU's OpenMP parallelization. More details about the GPU code public version and its performance are presented in Spurzem et al. 2012 and Berczik et al. 2013. The present code is well tested and has already been used to obtain important results in our earlier large scale (up to few million body) simulations, for more details see Khan et al. 2018, Panamarev et al. 2019, Shukirgaliyev et al. 2017 and Ernst et al. 2011.

2.2. *Initial parameter space*

We were looking for the best-fitting King models (King 1966) for the current observations from Gaia DR3. We assume that the clusters age is exactly 50 Myr. Our main goal was to reproduce the final cumulative mass profiles $M(\text{r})$ for both objects. For the Cr 135 we used the range within $0 < r < 20$ pc and for UBC 7 – $0 < r < 15$ pc. These limits correspond to the clusters' current Jacobi radii. Because the initial masses of the clusters are quite uncertain, we used for the modelling the initial masses as one of the initial fitting parameters. Since clusters are formed in molecular clouds with a low star formation efficiency, they are most probably supervirial after the initial gas expulsion phase (Shukirgaliyev et al. 2021). For the initial mass function we used the Kroupa 2001 approximation, with the lower mass $m_{\text{l}} = 0.1\ M_\odot$ and the upper mass $m_{\text{h}} = 10\ M_\odot$ limits. The other two main parameters for the cluster initial models was a R_{core} and the King concentration parameter W_0, individually for ach clusters (see Table 2). For the stellar metallicity we used the value $Z = 2\%$ (assumed as a Solar value) for both clusters.

For the initial positions and orbital velocities of the star clusters centre we used the selected `#(53,61)` model from our Kovaleva et al. 2020 paper. The initial conditions for the clusters center of mass coordinates and velocities are taken from this model (see Table 1).

More than 50 individual models with stellar evolution have been computed. The total running time for one typical model on a AMD 3600X 4.1 GHz CPU with a GeForce RTX 2600 Super GPU card was about 2 min. Minimizing the difference between the

Table 2. Initial values of physical parameters for Cr 135 and UBC 7.

| Cluster	$M_\odot$	N	R, pc	W_0
Cr 135	230	442	10	3
UBC 7	200	384	7	11
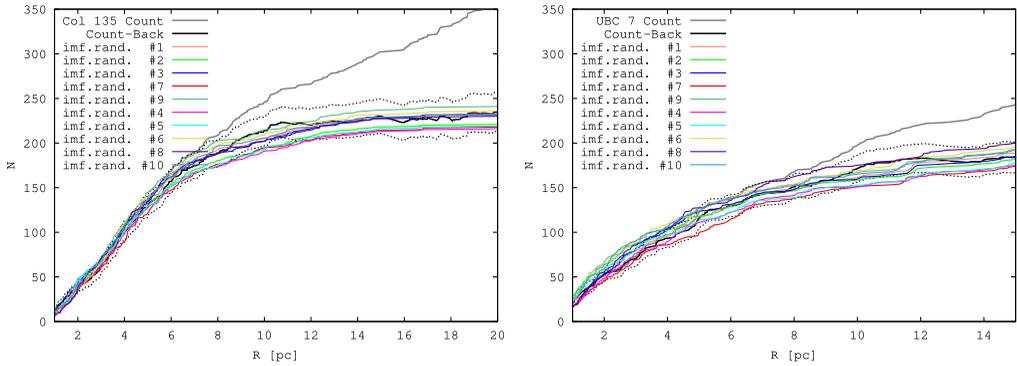
Figure 1. Cumulative number distribution of stars for clusters Cr 153 (left panel) and UBC 7 (right panel). The different color lines represents the set of randomization for initial mass function when the coordinates and velocities of the stars are fixed.
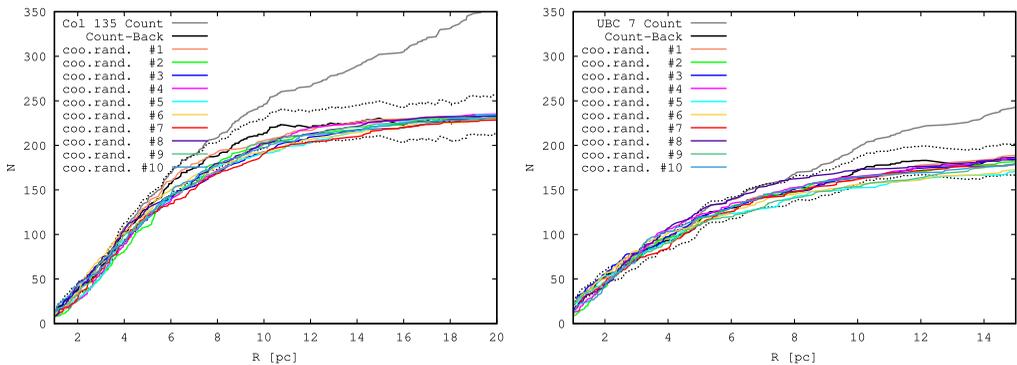
Figure 2. Same as Fig. 1 but randomization for initial coordinates and velocities was done with the fixed initial stellar mass function.

cumulative number distributions of the observed clusters and the numerical models we find simultaneously the best-fit parameters for both clusters, see Table 2.

After the first set of fitting procedure we run extra 20 more numerical models (with the same cluster physical parameters but using different randomization parameters). First we generated 10 random sets with different initial mass function (different color lines), keeping fixed the initial positions and velocities of the stars, see Fig. 1. For the second 10 random sets we used one selected initial mass function and randomize the stars positions and velocities (different color lines), see Fig. 2. On these figures we present as a black thick line the observed cumulative number distribution of stars for both clusters. The total cumulative number distributions of stars including the stellar background are presented on the figures as constantly growing gray lines. Because the observations have own limitations due to the Gaia satellite specifications, we select from the numerical models only the stars which are inside the specific stellar mass range - from 0.28 to 4.0 $M_\odot$. On our comparison figures we also exclude the neutron stars and black holes. The dotted gray lines on the figures represents the one $\pm\sigma$ difference levels from observed cumulative number distribution of stars.

Table 3. Comparison of position and velocity values for Cr 135 and UBC 7 center mass in Cartesian Galactic coordinates at 50 Myr with numerical simulation and observations.

Cluster	Type	X, pc	Y, pc	Z, pc	V_x, km/s	V_y, km/s	V_z, km/s
Cr 135	Sim	−8282.94	−284.32	−34.25	−7.65	237.32	−5.01
	Obs	−8282.14	−271.00	−36.16	−7.38	237.94	−4.85
UBC 7	Sim	−8284.14	−251.01	−45.80	−7.43	237.61	−4.65
	Obs	−8276.21	−250.87	−43.63	−7.00	238.13	−4.27
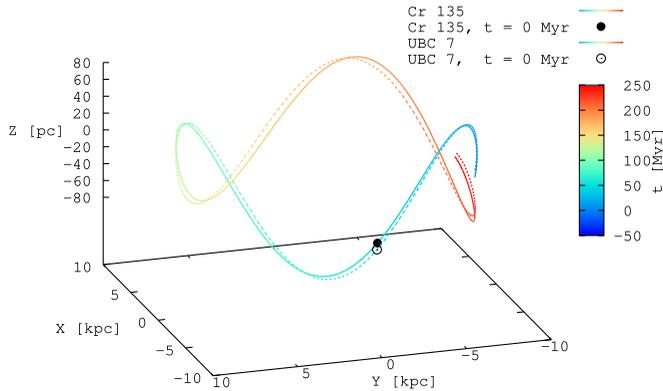
Figure 3. 3D orbits evolution of the Cr 135 (solid line) and UBS 7 (dotted line) up to 250 Myr. Black filled and black open circles are position of clusters at 0 Myr.

As we can see from figures Fig. 1 and Fig. 2 both sets of randomization of our best fitted physical model for clusters Cr 135 and UBC 7 are well inside the one $\pm\sigma$ gap.

3. Results

We present a numerical simulations using realistic star cluster N-body modelling by integrating a star-by-star cluster models in the analytic Milky Way potential to the present day. The code takes in to account up to date stellar evolution models (Banerjee et al. 2020). The average model relative errors between the observations and numerical simulations are better than 1%. This is a remarkable small error taking in account that the observational average line of site velocity error is around 10%.

The orbits integration with a simple integrator yielded the initial position of the Cr 135 ans UBS 7 at the time of their formation (see Table 1). The present-day position and velocity of the Cr 135 and UBC 7 obtained from numerical simulation are given in Table 3. The full 3D orbits of the evolution are shown in Fig. 3. It should be noted that the clusters rotate around each other during their orbital motion.

4. Conclusions

We present a numerical simulations using realistic star cluster N-body modelling by integrating a star-by-star cluster models in the analytic Milky Way potential to the present day. We were looking for the best-fitting King models for the observations from Gaia DR3 after 50 Myr of evolution. The comparative result of observational data and simulations for 50 Myr showed a fairly good agreement. The probability of a random coincidence chance is only about 2%.

5. Acknowledgements

References

Banerjee, S., Belczynski, K., Fryer, C. L., Berczik, P., Hurley, J. R., Spurzem, R., & Wang, L. 2020, BSE versus StarTrack: Implementations of new wind, remnant-formation, and natal-kick schemes in NBODY7 and their astrophysical consequences. *A&A*, 639, A41.

Beccari, G., Boffin, H. M. J., & Jerabkova, T. 2020, Uncovering a 260 pc wide, 35-Myr-old filamentary relic of star formation. *MNRAS*, 491(2), 2205–2216.

Beccari, G., Boffin, H. M. J., Jerabkova, T., Wright, N. J., Kalari, V. M., Carraro, G., De Marchi, G., & de Wit, W.-J. 2018, A sextet of clusters in the Vela OB2 region revealed by Gaia. *MNRAS*, 481(1), L11–L15.

Berczik, P., Spurzem, R., Wang, L., Zhong, S., & Huang, S. Up to 700k GPU cores, Kepler, and the Exascale future for simulations of star clusters around black holes. In *Third International Conference "High Performance Computing", HPC-UA 2013, p. 52–59* 2013, pp. 52–59.

Bisht, D., Zhu, Q., Yadav, R. K. S., Ganesh, S., Rangwal, G., Durgapal, A., Sariya, D. P., & Jiang, I.-G. 2021, Multicolour photometry and Gaia EDR3 astrometry of two couples of binary clusters (NGC 5617 and Trumpler 22) and (NGC 3293 and NGC 3324). *MNRAS*, 503(4), 5929–5947.

Cantat-Gaudin, T., Jordi, C., Wright, N. J., Armstrong, J. J., Vallenari, A., Balaguer-Núñez, L., Ramos, P., Bossini, D., Padoan, P., Pelkonen, V. M., Mapelli, M., & Jeffries, R. D. 2019,a Expanding associations in the Vela-Puppis region. 3D structure and kinematics of the young population. *A&A*, 626a, A17.

Cantat-Gaudin, T., Mapelli, M., Balaguer-Núñez, L., Jordi, C., Sacco, G., & Vallenari, A. 2019,b A ring in a shell: the large-scale 6D structure of the Vela OB2 complex. *A&A*, 621b, A115.

Castro-Ginard, A., Jordi, C., Luri, X., Julbe, F., Morvan, M., Balaguer-Núñez, L., & Cantat-Gaudin, T. 2018, A new method for unveiling open clusters in Gaia. New nearby open clusters confirmed by DR2. *A&A*, 618, A59.

Ernst, A., Just, A., Berczik, P., & Olczak, C. 2011, Simulations of the Hyades. *A&A*, 536, A64.

Gaia Collaboration, Prusti, T., de Bruijne, J. H. J., Brown, A. G. A., & et al. 2016, The Gaia mission. *A&A*, 595, A1.

Harfst, S., Gualandris, A., Merritt, D., Spurzem, R., Portegies Zwart, S., & Berczik, P. 2007, Performance analysis of direct N-body algorithms on special-purpose supercomputers. *NewAstr*, 12, 357–377.

Khan, F. M., Capelo, P. R., Mayer, L., & Berczik, P. 2018, Dynamical Evolution and Merger Timescales of LISA Massive Black Hole Binaries in Disk Galaxy Mergers. *ApJ*, 868(2), 97.

Kharchenko, N. V., Piskunov, A. E., Schilbach, E., Röser, S., & Scholz, R.-D. 2012, Global survey of star clusters in the Milky Way. I. The pipeline and fundamental parameters in the second quadrant. *A&A*, 543, A156.

King, I. R. 1966, The structure of star clusters. III. Some simple dynamical models. *AJ*, 71, 64.

Kovaleva, D. A., Ishchenko, M., Postnikova, E., Berczik, P., Piskunov, A. E., Kharchenko, N. V., Polyachenko, E., Reffert, S., Sysoliatina, K., & Just, A. 2020, Collinder 135 and UBC 7: A physical pair of open clusters. *A&A*, 642, L4.

Kroupa, P. 2001, On the variation of the initial mass function. *MNRAS*, 322(2), 231–246.

Nitadori, K. & Makino, J. 2008, Sixth- and eighth-order Hermite integrator for N-body simulations. *NewAstr*, 13, 498–507.

Panamarev, T., Just, A., Spurzem, R., Berczik, P., Wang, L., & Arca Sedda, M. 2019, Direct N-body simulation of the Galactic centre. *MNRAS*, 484(3), 3279–3290.

Pang, X., Li, Y., Tang, S.-Y., Pasquato, M., & Kouwenhoven, M. B. N. 2020, Different Fates of Young Star Clusters after Gas Expulsion. *ApJL*, 900(1), L4.

Shukirgaliyev, B., Otebay, A., Sobolenko, M., Ishchenko, M., Borodina, O., Panamarev, T., Myrzakul, S., Kalambay, M., Naurzbayeva, A., Abdikamalov, E., Polyachenko, E., Banerjee, S., Berczik, P., Spurzem, R., & Just, A. 2021, Bound mass of Dehnen models with a centrally peaked star formation efficiency. *A&A*, 654, A53.

Shukirgaliyev, B., Parmentier, G., Berczik, P., & Just, A. 2017, Impact of a star formation efficiency profile on the evolution of open clusters. *A&A*, 605, A119.

Spurzem, R., Berczik, P., Berentzen, I., Ge, W., Wang, X., Schive, H.-Y., Nitadori, K., & Hamada, T. Supermassive Black Hole Binaries in High Performance Massively Parallel Direct N-body Simulations on Large GPU Clusters. In Dubitzky, W., Kurowski, K., & Schott, B., editors, *Large Scale Computing Techniques for Complex Systems and Simulations* 2011,a, Wiley Publishers, pp. 35–58.

Spurzem, R., Berczik, P., Hamada, T., Nitadori, K., Marcus, G., Kugel, A., Männer, R., Berentzen, I., Fiestas, J., Banerjee, R., & Klessen, R. 2011,b Astrophysical Particle Simulations with Large Custom GPU Clusters on Three Continents. *Computer Science - Research and Development (CSRD)*, 26b, 145–151.

Spurzem, R., Berczik, P., Zhong, S., Nitadori, K., Hamada, T., Berentzen, I., & Veles, A. Supermassive Black Hole Binaries in High Performance Massively Parallel Direct N-body Simulations on Large GPU Clusters. In Capuzzo-Dolcetta, R., Limongi, M., & Tornambè, A., editors, *Advances in Computational Astrophysics: Methods, Tools, and Outcome* 2012, volume 453 of *Astronomical Society of the Pacific Conference Series*, 223.

Zhong, J., Chen, L., Kouwenhoven, M. B. N., Li, L., Shao, Z., & Hou, J. 2019, Substructure and halo population of Double Cluster h and χ Persei. *A&A*, 624, A34.

6. Discussion

Q: Thank you for presenting the simulation results. I have a question about how the comparison of the results of the simulation with the observational data was carried out? Such as figure 1 or 2 (Christian Boily) A: To compare our results with observational data, we performed a transformation of the galactocentric coordinates into equatorial coordinate system. (Marina Ishchenko)